Chapter 6. Electrical properties

6.1. Introduction

In this chapter, the studies of the electrical characteristics of molecular hybrid films based on rare earth metal quinoline complexes (Req_3) as thin films are presented. Basically, almost all organic solids are insulators. However, when their constitute molecules have a π-conjugate (π*) systems, the electrons will move via π electron cloud overlap by hopping, tunneling and other related mechanisms. As the result, the electric charge (holes and electrons) can flow in the organic materials and thereby exhibits the semiconductor properties. Charge transfer complexes are one of the major classes of organic semiconductor material. It often demonstrates a similar conduction behavior as inorganic semiconductor. With this features, Req_3 ternary complexes had become the suitable candidate that can demonstrate a good semiconducting properties.

Despite of its fascinating semiconducting nature, Req_3 also has proven to exhibit luminescent property. On the basis of its luminescence characteristics, Req_3 has been applied as the active material in organic light emitting device (OLED). For this purpose, indium tin oxide (ITO) is normally used as the transparent electrode. The luminosity is measured using Konica Minolta CS-200 chromameter which can be measured as low as 0.01 cd/m^2 while programmable Keithley 2400 SMU (source measurement unit) is used to source the supply voltage and measures the resulting current of the device.

Additionally, the charge transport mechanism of the device is also evaluated since it is one of the main factors that are affecting the device characteristics. Basically there are two different charge mechanisms, contact limited and bulk limited which can be used to describe the electrical characteristics of the organic semiconductor. Deep understanding on the basic charge conduction mechanism is important as it will help to distinguish the influence of the interfacial or bulk effects on the electrical properties of these devices.

The basic parameters that control the devices performances are also investigated. The Shockley diode equation is applied to extract the electronic parameters of ITO/Req_3 ternary complexes/Al devices. Two different methods which are conventional ln I-V and Cheung's functions, are utilized to determine the electronic parameters of the diode such as the ideality factor, n, effective barrier height, Φ_b, and saturation current, I_0. These are the two established method that have been used to extract the electronic parameters for the organic semiconductor devices as reported by many researcher (Boyarbay, Çetin, Kaya, & Ayyildiz, 2008; Farag, Farooq, & Yakuphanoglu, 2011; Güllü, Çankaya, Biber, & Türüt, 2008; Günsel, Kandaz, Yakuphanoglu, & Farooq, 2011; Shah, Sayyad, & Karimov, 2011); (Aydin, Farag, Abdel-Rafea, Ammar, & Yakuphanoglu, 2011; Farag, et al., 2011; Wetzelaer, Koster, & Blom, 2011) . Generally, knowledge concerning the electronic parameters is important as it will help to investigate the electrical properties of each organic material.

6.2. Electrical analysis for single layer OLED device with ITO/Euq_3 ternary complexes/Al structure (Europium as the metal centre)

6.2.1. I- V characteristics of ITO/Euq_3 ternary complexes/Al structure

The basic mechanism of OLED has been established to be in three steps which are charge injection, charge transport and recombination process. From the viewpoint of the charge transport and injection, the turn on voltage in the current-voltage characteristics of the device is one of the most important parameter to describe the performance of an OLED (Wu et al., 2010). However, there are two different definitions of the turn on voltage. According to Wu et al., in some study, the turn on voltage is defined as the bias voltage at which the current increases drastically to a certain voltage (Wang et al., 2004; Wu, et al., 2010) whereas the other reports defined the turn on voltage as the bias voltage at which the luminescence device reaches 1 cd/m^2 (Binnemans, 2005; Chan, Lai, Fung, Lee, & Lee, 2004; Wu, et al., 2010; Xie et al., 2008; Yap, Yahaya, & Salleh, 2008). In this study, the objective of fabricating a single layer OLED was not meant to obtain an optimum efficient device, but to focus on the analysis of the electrical characteristics of the device. Therefore, in this investigation, the turn on voltage is defined as the voltage where the current demonstrates a rapid rise and starts to increase drastically (Wu, et al., 2010).

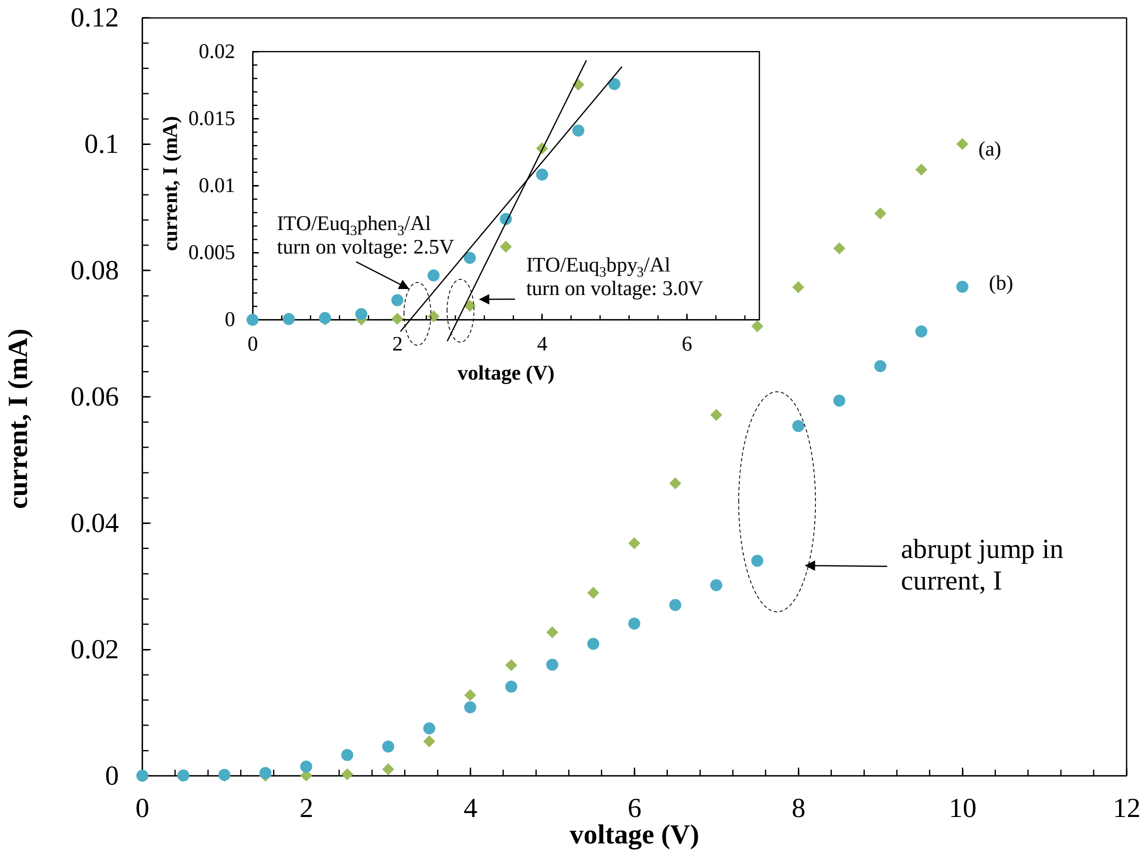

Figure 6.1 I- V characteristics of single layer devices of (a) ITO/Euq_3bpy_3/Al (b) ITO/ Euq_3phen_3/Al

The I-V measurements were performed on the single-layer devices with the configuration ITO/Euq_3bpy_3/Al and ITO/Euq_3phen_3/Al. From Figure 6.1, it can be seen that, by applying voltage across the devices, the current, I increases exponentially with the turn on voltage of 3.0 ± 0.1 V and 2.5 ± 0.1 V for ITO/Euq_3bpy_3/Al and ITO/ Euq_3phen_3/Al devices respectively. Basically, the turn on voltage is obtained from the linear fit method where a tangent line is drawn along the current and voltage curves (I-V curves) on the rising part and extends until it intersect with the horizontal voltage axis (E. Farsad, 2011). This part has been enlarged and shown as the inset of Figure 6.1. The turn on voltage obtained from ITO/Euq_3bpy_3/Al is found to be slightly higher compares to that of ITO/Euq_3phen_3/Al device. The decreased turn on voltage in the ITO/ Euq_3phen_3/Al device can be attributed to the better carrier mobility which enables balance charge transport. From this result, it is seen that the variation of the neutral ligand in the Euq_3 ternary complexes may cause a slightly change in the turn on voltage. However, an anomalous behavior concerning a gradual increased in current, *I*, at 7.5 ± 0.1 V for ITO/Euq_3phen_3/Al device is observed. The instability of the I-V curves which is detected from the abrupt current jump is probably arise from the structural defect of the Euq_3phen_3 ternary complex film which might be formed during the measurement (Woo et al., 2001). Additionally, it is also observed that both devices ITO/Euq_3bpy_3/Al device exhibits the highest current, I of 0.10 ± 0.01 mA at 10.0 ± 0.1 V while ITO/ Euq_3phen_3/Al device produces the highest current, *I* of 0.08 ± 0.01 mA at 10.0 ± 0.1 V. Nevertheless, compared to the other conventional OLED, the current values are still significantly very low. One of the possible reasons is might due to the poor transportation of hole and electrons in the organic layer that causes inefficient charge transportation in the devices.

It is well worth to note that the luminosity, *L*, of the device is measured simultaneously with the current voltage characteristics. It is established that OLED with europium complexes as the emitting layer will emit a red colour. However, such light emission colour is not expected to be observed from these devices. This is because it has been proven in the PL analysis that these Euq_3 ternary complexes will exhibit yellowish green emission due to the significant ligand peak in the PL spectra which overshadows the metal emission since the energy transfer that occurs from the ligand to the metal Eu^{3+} ion is inefficient. As a result, there was no obvious light emission captured in these single layer devices. The other factor which contribute to the low luminance is due to the fact that the device structure that consists of only an emitting organic layer. The absence of a hole and an electron transports layer causes an imbalance in the carrier transport and, thus, results in charge accumulation at the interface. Charge accumulation leads to exciton quenching (Kappaun, Slugovc, & List, 2008). This is supported by the aforementioned current, which shows lower values. In order to enhance the luminosity, the devices require a charge transport material to be inserted between the cathode and the layer of europium complex such that charge injection can be facilitated and the recombination of the electrons and holes in the emitting layer can be enhanced.

6.2.2. Charge transport mechanism of ITO/Euq_3 ternary complexes/Al structure: Contact limited versus bulk limited

Additional analysis of the I-V curves is performed. It is known that the dynamics of the I-V measurement can give insight into the transport mechanism that exists in the ITO/Euq_3bpy_3/Al and ITO/Euq_3phen_3/Al devices. Basically there are two type of transport mechanisms that has been established to occur in the device which is known as the charge injection from the electrode (contact limited) and charge transport through the organic/bulk layer (bulk limited). Basically, Richardson-Schottky thermionic emission and Fowler-Nordheim tunneling are considered as the mechanisms that describe the contact limited phenomena. On the other hand the band conduction model theories which are used to describe charge conduction in the bulk are ohmic, space charge limited current (SCLC), trap charged limited current (TCLC) and trapped filled space charge limited current (TFSCLC) as well as Poole-Frenkel mechanism.

One of the methods that can be used to predict the presence of the bulk limited in the devices is by fitting the I-V according to the power law relation describes by, $I \backsim V^m$ where m is used to determine the slope of the double logarithmic plot of the I-V characteristics. Figure 6.2 and 6.3 show the double logarithmic I-V plot for ITO/Euq_3bpy_3/Al and ITO/Euq_3phen_3/Al respectively in which three distinct regions are identified. In region I (low voltage region), the slope of logarithmic J-V curves is approximately 1.6 and 1.9 for Euq_3bpy_3 and Euq_3phen_3 complexes respectively. This region is considered as being reasonable for describing the space charge limited current (SCLC) mechanism. At region II, as the voltage increases, the space charge effect is negligible due to the large electric field that causes a large injected charge carrier. The large charge carriers are then trapped within the Euq_3bpy_3 and Euq_3phen_3 bulk material and cause a rapid increase in the current. The m value which is obtained from the slope of the logarithmic I-V curves in the higher voltage region (region II) is found to be approximately 6.9 and 3.2 for ITO/Euq_3bpy_3/Al and ITO/Euq_3phen_3/Al respectively. This behavior is classified as trap charged limited current (TCLC). In region III, as the voltage rises, the injected charge carrier started to fill up all the trap sites within the Euq_3bpy_3 and Euq_3phen_3 bulk material, the additional injected charge carrier seems to move freely. Therefore this region is contributed to the trapped filled space charge limited current (TFSCLC) in which the slope determined in the logarithmic I-V curves is approximately 2.3 and 2.1 for Euq_3bpy_3 and Euq_3phen_3 complexes respectively.

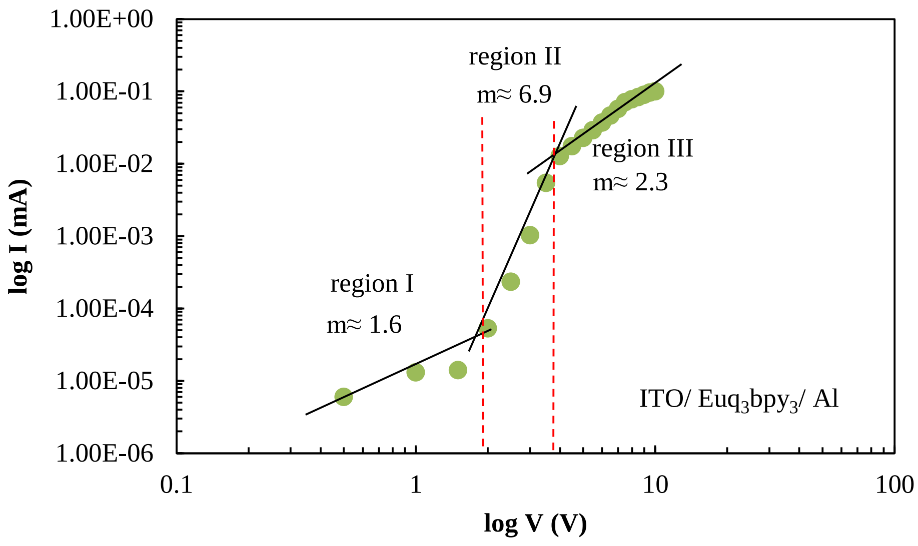

Figure 6.2 Logarithmic plot of I- V characteristic of ITO/Euq_3bpy_3/Al

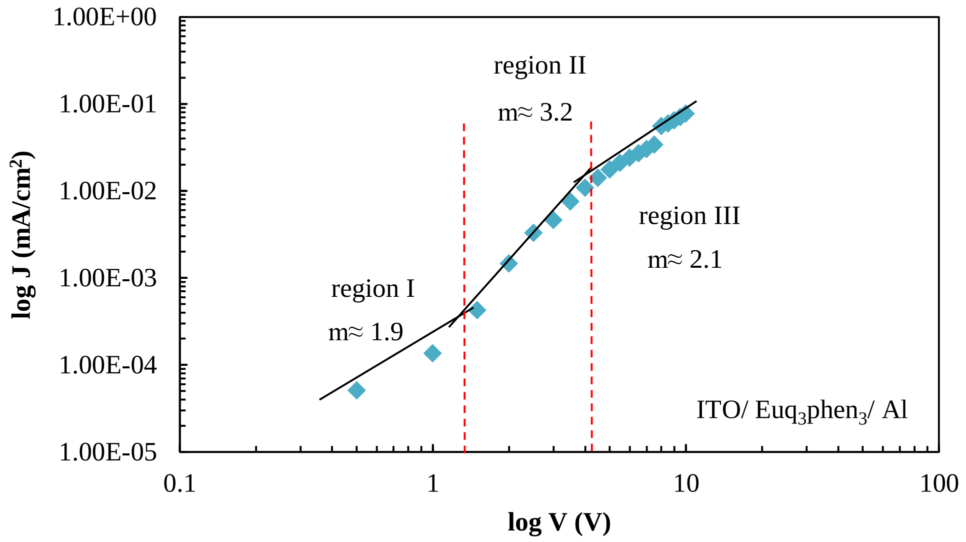

Figure 6.3 Logarithmic plot of I- V characteristic of ITO/Euq_3phen_3/Al

Even though, the behavior demonstrates from both devices indicated the bulk limited, the maximum SCLC effect is still not observed. According to Riechel, in order to achieve the maximum SCLC effect, it is essential to have the ohmic contact which means that the electrodes must be able to supply more carriers per unit time than can be transported through the organic layer (Riechel, 2002). However, there is no ohmic conduction detected in from this double logarithmic I-V plot in which supposedly is reflected by slope of 1. This behavior reveals that the dominance of the transport mechanism could not be taken as bulk limited since the effect of SCLC was not maximum. However it should be noted that this is just a simple estimation to predict the dominance of the transport mechanisms exist in the devices. In order to support this prediction, other factors such as temperature and thickness dependence should be considered as well (Baldo & Forrest, 2001; Brütting, Berleb, & Mückl, 2001; Khalifa, Vaufrey, Bouazizi, Tardy, & Maaref, 2002). However, such investigation has not been carried out in this research. Therefore, it is reasonable to make an earlier prediction that the bulk limited is not dominance in these devices.

By assuming that the injection at metal and organic layer interface is thermally activated at the room temperature, the Richardson- Schottky (R-S) thermionic emission has been considered as the transport characteristics at the contact (Baldo & Forrest, 2001). The R-S model underlying assumptions as described by the following equation (Brütting, et al., 2001)

$$I_{R-S} = A^{*}T^{2}\exp\left(\frac{\beta_S E^{\frac{1}{2}} - q\varphi_b}{kT}\right) \qquad (6.1)$$

where $I_{R\text{-}S}$, is the R-S current, $\beta_S = \left(\frac{q^3}{4\pi\varepsilon_o\varepsilon}\right)^{\frac{1}{2}}$, A^* is the Richardson constant, q is the electron charge, ε_o is the vacuum dielectric permittivity, k is the Boltzmann constant, T is the temperature, φ_b is the Schottky contact potential barrier height and ε is the organic semiconductor dielectric permittivity. According to Equation 6.1, the presence of the R-S thermionic emission in the ITO/Euq_3bpy_3/Al and ITO/ Euq_3phen_3/Al devices can be identified from the linear dependence of $ln\ I \sim V^{1/2}$ in the lower voltage region. It is clear in this figure that the thermionic emission model fit well to the low voltage as shown in Figure 6.4. This behavior indicates that the transport mechanism is the contact limited behavior. It should be noted the R-S plot in this part has not been further analyzed as it only meant to predict the presence of the R-S effect in the devices. Another things that should be highlighted is that despite of different neutral ligand that had been attached to the Euq_3 ternary complexes, both devices still demonstrate the same transport mechanism. The transport behavior does not depends on the properties of the Euq_3 ternary complexes which further support the dominance of the contact limited effect but not the bulk limited effect .

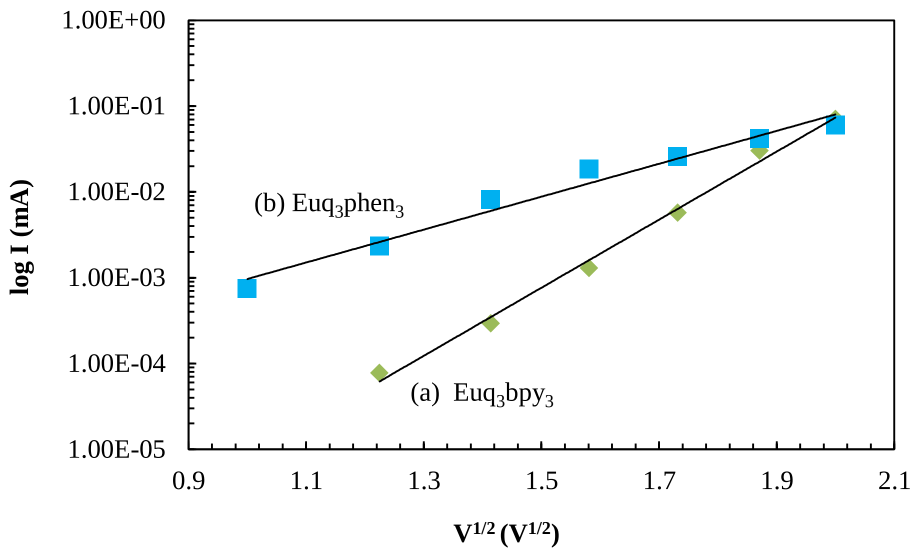

Figure 6.4 Richardson-Schottky (R-S) plot of I- V characteristics of (a) ITO/Euq_3bpy_3/Al and (b) ITO/Euq_3phen_3/Al

6.2.3. Evaluation of electronic parameters for the ITO/Euq_3 ternary complexes/Al structure

From the above analysis, it is obvious that the charge transport mechanism in the ITO/Euq_3 ternary complexes/Al is predominantly a Richardson-Schottky type conduction mechanism. This suggests that Schottky barrier is formed between the Euq_3 ternary complexes and aluminum electrode junction. For further analysis of the I-V characteristics, the Shockley diode equation is applied to extract the electronic parameters of ITO/Euq_3 ternary complexes/Al devices. The Shockley equation is described by a relation that considered the thermionic emission at the junction interface (Günsel, et al., 2011). It should be noted that the equations used in these investigations have been derived for inorganic semiconductors with well-defined band structure (Blom & Vissenberg, 2000; Brütting, et al., 2001). For organic semiconductors with an energy distribution of localized states (Bässler, 1998), the analysis is expected to be more complicated (Arkhipov, Emelianova, Tak, & Bässler, 1998; Conwell & Wu, 1997). However, many researchers in the field of the organic semiconductors have applied this equation to describe the current-voltage characteristics and also to predict the materials behavior (Aydin, et al., 2011; Farag, et al., 2011; Wetzelaer, et al., 2011) . The exponential expression of the Shockley equation is expressed as (Boyarbay, et al., 2008).

$$I_0 = I_0 exp\left(\frac{qV}{nkT}\right)[1 - \exp\left(-\frac{qV}{kT}\right)] \quad (6.2)$$

where V is the voltage, I is the current, I_0 is the saturation current, n is the ideality factor, k is the Boltzmann constant, T is the temperature, q is the electronic charge and R_s is the series resistance. The saturation current, I_0 is determined by (Boyarbay, et al., 2008; Farag, Ashery, Terra, & Mahmoud, 2008),

$$I_0 = AA^{*}\exp(-\frac{q\Phi_b}{kT}) \quad (6.3)$$

where A is the geometrical area of the diode, A^* is the effective Richardson constant which is equal to 120 A $cm^{-2}K^{-2}$ and Φ is equal to the barriers height.

The semi-logarithmic I-V plots of ITO/Euq_3 ternary complexes/Al devices are shown in Figure 6.5. As indicated in this figure, the log I-V characteristics are classified into two regions with respect to their applied voltage. The exponential increase of the current at the lower voltage (region I) may be attributed to the decrease in the depletion region layer at the junction interface which leading to rectifying properties (Güllü, et al., 2008; Günsel, et al., 2011; Shah, et al., 2011). In region II, the current starts to deviates from the exponential due to the effect of series resistance, R_s from the contact wires or bulk resistance of the organic layer, the interfacial layer and the interfaces state, in which giving rise to the downward concave curvature in the semi-logarithmic I-V characteristic (Farag, et al., 2011; Güllü, et al., 2008).

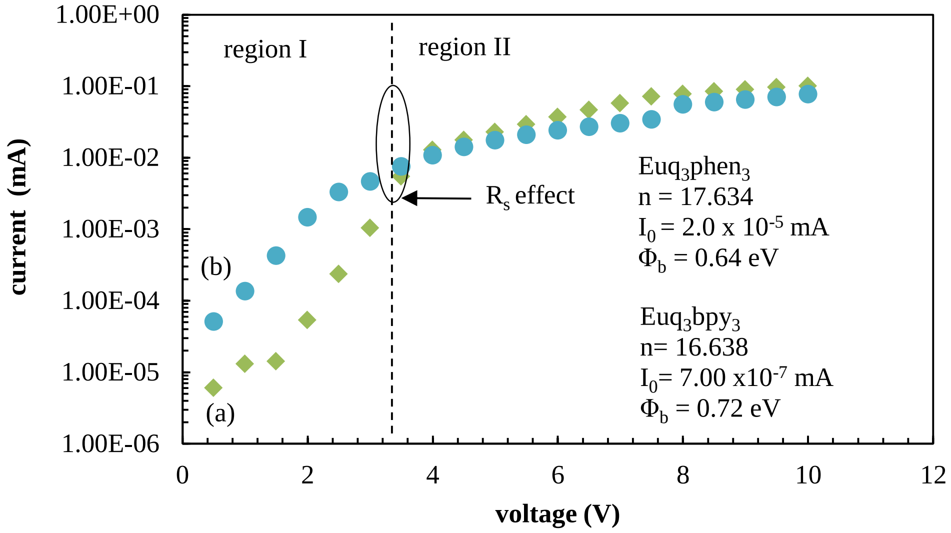

Figure 6.5 I- V characteristics (I- V) of single layer devices of (a) ITO/Euq_3bpy_3/Al and (b) ITO/ Euq_3phen_3/Al

The non-ideal behavior exhibited by these devices plays a significant role in the determination of the electronic parameters of the diode such as the ideality factor, n, effective barrier height, Φ_b and saturation current, I_0 (Günsel, et al., 2011). According to A.A.M. Farag, the exponential behavior of the semi-logarithmic I-V characteristics depends on the property of organic material used in the devices (Farag, et al., 2011). As support to that, the experimentally measured I-V characteristic often demonstrate a more complex behavior compare to the ideal diode due to the different effect such as series resistance and various conduction mechanism (Aydin, et al., 2011) . Therefore the electronic parameters of the diodes will give a rough prediction of the electrical properties of Euq_3 ternary complexes used in these devices due to their influence in the exponential behavior of the semi-logarithmic I-V characteristics.

The ideality factor, *n* is one of the diode parameter that affects the exponential behavior of the semi-logarithmic I-V characteristics (Farag, et al., 2011) .It is a measure of how close the diode follows the ideal diode equation. It is introduced to calculate the deviation of the experimental I-V data from the ideal thermionic model (Aydin, et al., 2011). It is well known that the ideality factor *n*, should be unity in order to obtain an ideal model. According to thermionic emission theory (Rhoderick & Williams, 1988; Sze & Ng, 1981), the ideality factor could be determined from the slope of the linear regions (region I) of the semi-logarithmic I-V plot (Aydin, et al., 2011; Güllü, et al., 2008), given by (Boyarbay, et al., 2008; Farag, et al., 2008),

$$n = \frac{q}{kT}\frac{dV}{d(\ln I)} \tag{6.4}$$

The values of the ideality factor for the ITO/Euq_3bpy_3/Al and ITO/Euq_3phen_3/Al have been calculated as 16.638 ± 0.004 and 17.634 ± 0.001 respectively. These values appear to deviate with the ideal model which should be equal to the unity. The deviation of the value from unity is caused by several factors. Tung et al attributes the deviation of the value from unity to the presence of wide distribution of low Schottky effective barrier height patches caused by lateral inhomogeneity (Tung, 1992). Additionally, the other factors such as the fabrication-induced defects at the interface, the recombination of holes and electrons in the depletion region as well as the increase of the diffusion current due to the applied voltage may also considerably lead to an ideality factor greater than unity (Aydin, et al., 2011; Tung, 1992). The second parameter that should be highlighted is the saturation current, I_0. Generally it is determined from the intercept of the exponential part of the linear region (region I) of semi-logarithmic I-V characteristics. The saturation current, I_0 reflects the number of charges that are abled to overcome the barrier (Aydin, et al., 2011; Boyarbay, et al., 2008; Farag, et al., 2008; Farag, et al., 2011; Günsel, et al., 2011) The saturation current, I_0 for ITO/Euq_3bpy_3/Al and ITO/Euq_3phen_3/Al are found to be (7.0 ± 0.1) x10^{-7} mA and (2.0 ± 0.1) x10^{-5} mA respectively. The third parameter which is the effective barrier height, Φ_b is obtained from Equation 6.3,

$$q\Phi_b = \mathrm{kT}\ln\left(\frac{A^*AT^2}{I_0}\right) \tag{6.5}$$

The calculated effective barrier height, Φ_b for Euq_3bpy_3/Al and Euq_3phen_3/Al junctions are found to be 0.72 ± 0.03 eV and 0.64 ± 0.08 eV respectively. According to Boyarbay, the effective barrier height, Φ_b is expected to be correlated with the ideality factor (Boyarbay, et al., 2008). In this finding, the inverse relationship between the effective barrier height, Φ_b and the ideality factor, n is observed. This behavior appears to be in agreement with various reported work (Ahmad & Sayyad, 2008; Bandyopadhyay, Bhattacharyya, & Sen, 1999; Boyarbay, Çetin, Uygun, & Ayyildiz, 2011; Schmitsdorf, Kampen, & Mönch, 1997) .

Despite of applying the conventional I-V method, the diode parameters of an organic semiconductor can also be evaluated from the method develop by Cheung and Cheung which is known as Cheung's function (Cheung & Cheung, 1986) . The Cheung's function is expressed as:

$$\frac{\partial V}{\partial(\ln I)} = IR_S + n\frac{kT}{q} \tag{6.6}$$

$$H(I) = V - n\frac{kT}{q}ln\frac{I_0}{AA^*T^2} \tag{6.7}$$

and,

$$H(I) = IR_s + n\Phi_b \tag{6.8}$$

where the R_s is the series resistance, n is the ideality factor and Φ_b is the effective barrier height calculated from the I-V characteristics.

Figure 6.6 demonstrate the plots of dV/d(ln I)-I as obtained from the measurement of Cheung's functions. The slope of the dV/d(ln I)-I represent R_s while the y-axis intercept will give the nkT/q value (Farag, et al., 2011; Shah, et al., 2011). The obtained values for series resistance, R_s for ITO/ Euq_3bpy_3/Al and ITO/ Euq_3phen_3/Al were found to be 24.7 ± 0.3 kΩ and 59.3 ± 0.4 kΩ respectively. Also, the ideality factor, n is obtained as 11.689 ± 0.003 and 11.756 ± 0.001 for ITO/Euq_3bpy_3/Al and ITO/Euq_3phen_3/Al respectively. It is noteworthy that the ideality factor obtained from the dv/d(ln I)-I plot is slightly difference compare to that of the conventional I-V method. This deviation of the values may be due to the presence of the series resistance, interface states and the voltage drop across the interfacial layer (Shah, et al., 2011).

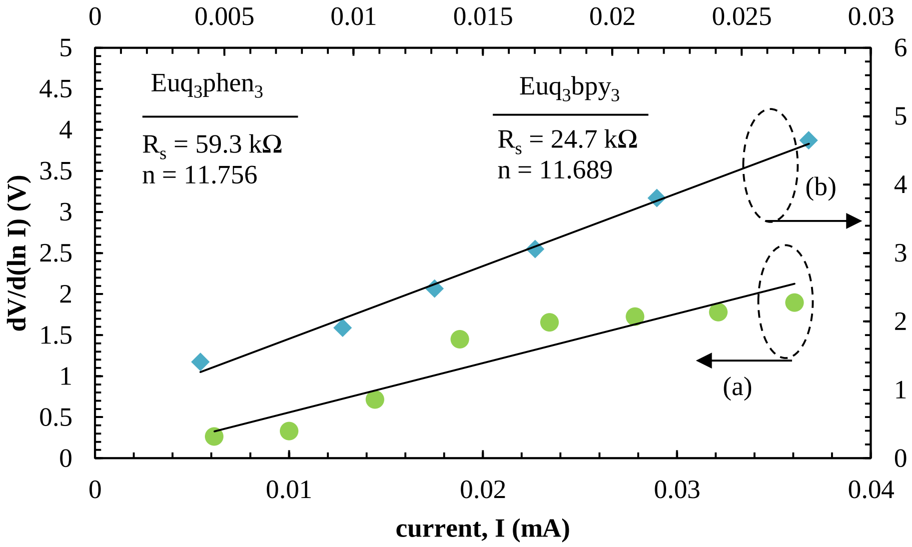

Figure 6.6 dV/d(lnI)-I plot of single layer devices of (a) ITO/Euq_3bpy_3/Al and (b) ITO/ Euq_3phen_3/Al

The obtained ideality factor n, estimated from the dV/d (ln I)-I plot was then used to plot H(I)- I as shown in Figure 6.7. According to Equation (6.8), the slope of the plot will reveal the values of the series resistance, R_s while the y-axis intercept is equal to $n\Phi_b$ (Farag, et al., 2011; Shah, et al., 2011). The series resistance value for ITO/ Euq_3bpy_3/Al and ITO/Euq_3phen_3/Al were found to be 28.7± 0.5 kΩ and 61.9± 0.5 kΩ. It is noticeable that series resistance, R_s values determined from the H(I)-I plot are approximately the same as aforementioned dV/d(lnI)-I plot. This indicates the consistency of the Cheung's functions for the determination of the series resistance, R_s. On the other hand, the effective barrier heights, Φ_b, obtained for ITO/Euq_3bpy_3/Al and ITO/ Euq_3phen_3/Al were found to be 0.79± 0.03 eV and 0.68 ± 0.02 eV respectively. From this finding, it is seen that the obtained values for the effective barrier height, Φ_b of both devices are approximately close to the values measured from the conventional I-V method which further support the consistency of the Cheung's function in determining the effective barrier height, Φ_b.

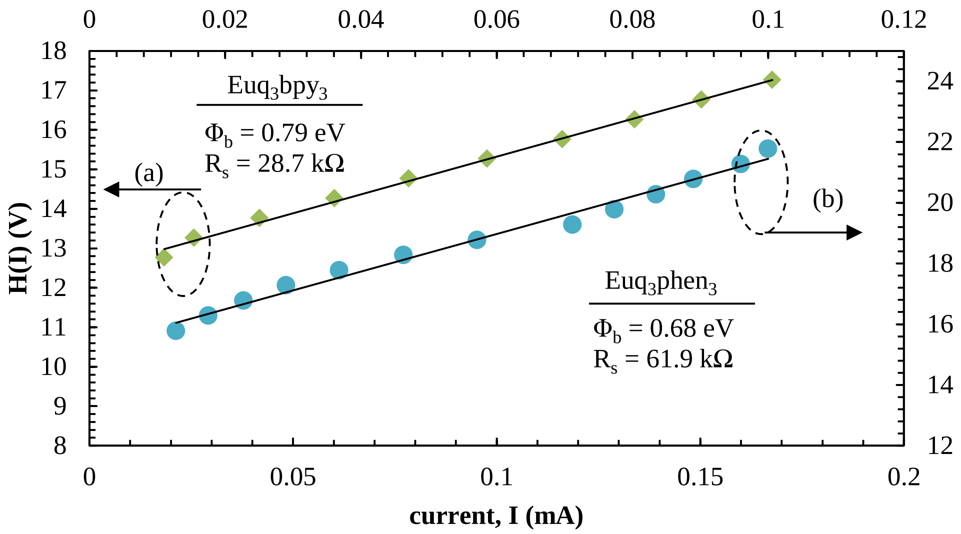

Figure 6.7 H(I)-I plot of single layer devices of (a) ITO/Euq_3bpy_3/Al and (b) ITO/Euq_3phen_3/Al

For clarification, all the diode parameters extract from both conventional I-V method and Cheung's function is tabulated in Table 6.1. By looking closely into the parameters extracted from the I-V characteristics that are tabulated in Table 1, one could notice that the saturation current, I_0 obtained from both complexes are appeared very high. One of the possible reasons may be contribute to the vital role of the minority carrier in these devices in which should be small compare to the majority carrier in order to have an ideal diode. This actually explains the failure in operation of the device as OLED. Normally, for the organic semiconductor, the I_0 should be around 10^{-10}- 10^{-12} in which should only depends upon thermal excitation of minority carriers.

Table 6.1 Various parameters extracted from the I-V characteristics of ITO/Euq_3phen_3/Al and ITO/ Euq_3bpy_3/Al

Diode parameter	ln I- V method		Cheung's functions			
			dV/d(ln I) - I		H(I)-I	
	Euq_3phen_3	Euq_3bpy_3	Euq_3phen_3	Euq_3bpy_3	Euq_3phen_3	Euq_3bpy_3
I_0 (mA)	(2.0 ± 0.1) x 10^{-5}	(7.0 ± 0.1) x 10^{-7}	-	-	-	-
Φ (eV)	0.64 ± 0.08	0.72 ± 0.03	-	-	0.68± 0.02	0.79± 0.03
n	17.634 ± 0.001	16.638 ± 0.004	11.756 ± 0.001	11.689 ± 0.003	-	-
R_s (kΩ)	-	-	59.3± 0.4	24.7 ± 0.3	61.9± 0.5	28.7± 0.5

Other than that, it is also noticeable that both complexes demonstrate deviation of ideality factors, *n* far from unity. However the corresponding values are still consider reasonable as the ideality factor obtained by other researchers for the organic semiconductor materials is usually reported in the range 1.7 to 45.0 in which depend on the properties of the organic semiconductor (Elmansouri et al., 2009; Farag, Haggag, & Mahmoud, 2012; Günsel, et al., 2011; Osiris, Farag, & Yahia, 2011; Shah, Sayyad, Karimov, & Maroof-Tahir, 2010; Shah, Sayyad, Karimov, & Wahab, 2010; Zorba, Watkins, Yan, & Gao, 2001). The reason of this deviation is previously explained.

Another thing that should be highlighted is the effective barrier height, Φ_b yield by both devices is also too high to allow injection current from the contact to the organic layer. Therefore it is insufficient to deliver the maximum possible SCLC in the material. In order to sustain the steady state SCLC, an ohmic contact is require to form between the electrode in the organic interface (Chiguvare, Parisi, & Dyakonov, 2003). According to Chrone, in order to achieve an ohmic contact, the effective barrier height, Φ_b must be at least less than 0.3 eV (Crone, Davids, Campbell, & Smith, 1998). However, such effective barrier height, Φ_b has not been observed. It further confirm that the transport behavior in these devices is dominated by the contact-limited transport model and not by the bulk limited as has been predicted in the last section.

Using the predicted effective barrier height, Φ_b and the band gap value obtained from Chapter 5, the HOMO and LUMO for both devices can be estimated. The schematic band diagram that corresponds to the estimated HOMO and LUMO values is proposed and shown in Figure 6.8. From the band diagram, one could notice that the barrier height between the ITO and HOMO level for ITO/Euq_3bpy_3/Al and ITO/Euq_3phen_3/Al were found to be 1.64 eV and 1.70 eV. These values are considered very high to allow efficient injection from the electrode into the bulk material. According to Qin, in order to have an efficient injection, the injection barrier height Φ_b, must always be less than 0.5 eV (Qin et al., 2012). This evidenced that the estimated barrier height Φ_b, is not an appropriate barrier for an efficient hole injection which consequently will cause the number of injected holes is less than electrons. As a result, imbalanced charge carrier injection or carrier mobility occur which lead to the reduction of the recombination rate of electrons and holes in the organic layer (Jiao et al., 2011). Consequently, the efficiencies of OLED which usually will depends on the recombination rate will decrease due to the occurrence of the exciton quenching processes close to the electrodes or non-radiatiave recombination of charges at the electrodes (Kappaun, et al., 2008). This would be one of the reasons that contribute to the OLED failure in these devices. This explanation also serves as a support to the domination of the contact-limited transport mechanism in these devices.

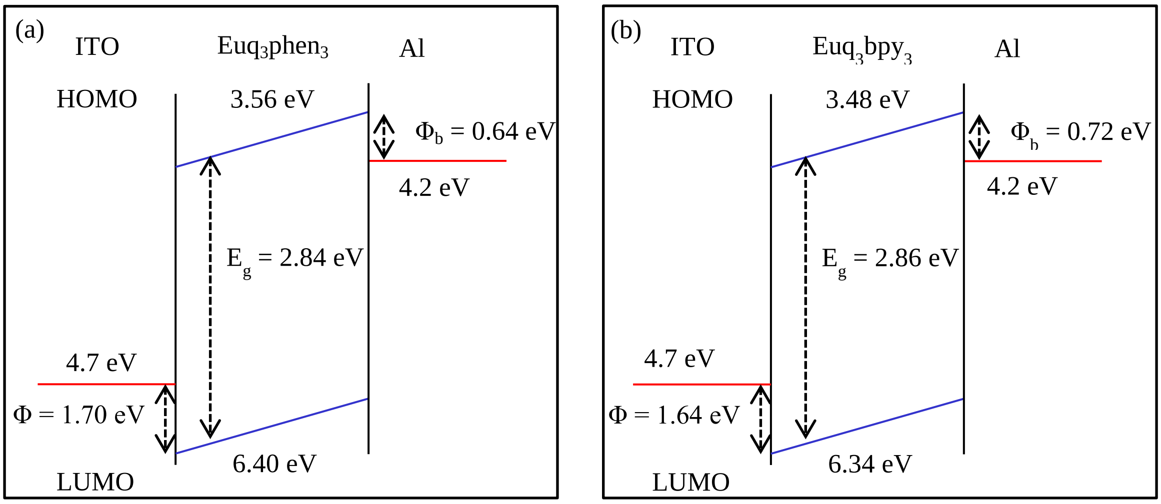

Figure 6.8 Schematic band diagram of (a) ITO/ Euq_3phen_3/Al and (b) ITO/ Euq_3bpy_3/Al after contact

Besides, there is an inverse relationship between the effective barrier height, Φ_b and the ideality factor, *n*. The ideality factor, *n* is found to increase as the effective barrier height, Φ_b decreases. Boyarbay attribute the linear relationship between the effective barrier height, Φ_b and the ideality factor, *n* to the lateral inhomogeneity's of the effective barrier height, Φ_b in the devices (Boyarbay, et al., 2008). However such effect seems not to be prominent in these two devices. The reason for this deviation is hard to explain. However, the plausible reasons may be attributed to many factors such as the fabrication-induced defects at the interface, the recombination of holes and electrons in the depletion region as well as the increase of the diffusion current due to the applied voltage.

It also can be observed that the ideality factor, *n* of ITO/Euq_3phen_3/Al is higher compares to ITO/Euq_3bpy_3/Al. According to Gullu, one of the factor that is attributed to the larger value of the ideality factor, *n* might be due to the existence of the series resistance, R_s in the interfacial layer (Güllü, et al., 2008). Therefore it is reasonable to attribute the higher ideality factor *n*, obtain for ITO/Euq_3phen_3/Al is due to higher series resistance, R_s of the ITO/Euq_3phen_3/Al compared to that of ITO/Euq_3bpy_3/Al. This indicates that that the adduction of Phen as the neutral ligand will cause the enhancement of the ideality factor n, as well as the increase in series resistance, R_s compared to that of Bpy ligand.

Another thing that should be highlighted is that the adduction of different neutral ligand is found to affect the electrical properties of these devices. Therefore it can be observed that the electronic parameters extracted from the I-V measurement is different as the adduction of the neutral ligand is changed. This also serves as support to the aforementioned statement by Farag in which has stated that I-V characteristics depends on property of organic material used in the devices (Farag, et al., 2011).

6.3. Electrical analysis for single layer OLED device with ITO/Tbq_3 ternary complexes/Al structure (Terbium as the metal centre)

6.3.1. I-V characteristics of ITO/Tbq_3 ternary complexes/Al structure

The I-V measurements of Tbq_3bpy_3 and Tbq_3phen_3 complexes are performed on the single-layer devices with the configuration ITO/Tbq_3bpy_3/Al and ITO/Tbq_3phen_3/Al.

Figure 6.9 shows the I-V curves obtained from the measurements. It is cleared in this figure that both devices demonstrate a typical diode curve with a turn voltage occur at 6.6 ± 0.1 V and 7.0 ± 0.1 V for ITO/Tbq_3bpy_3/Al and ITO/Tbq_3phen_3/Al devices respectively. This part has been enlarged and shown as the inset of Figure 6.8.

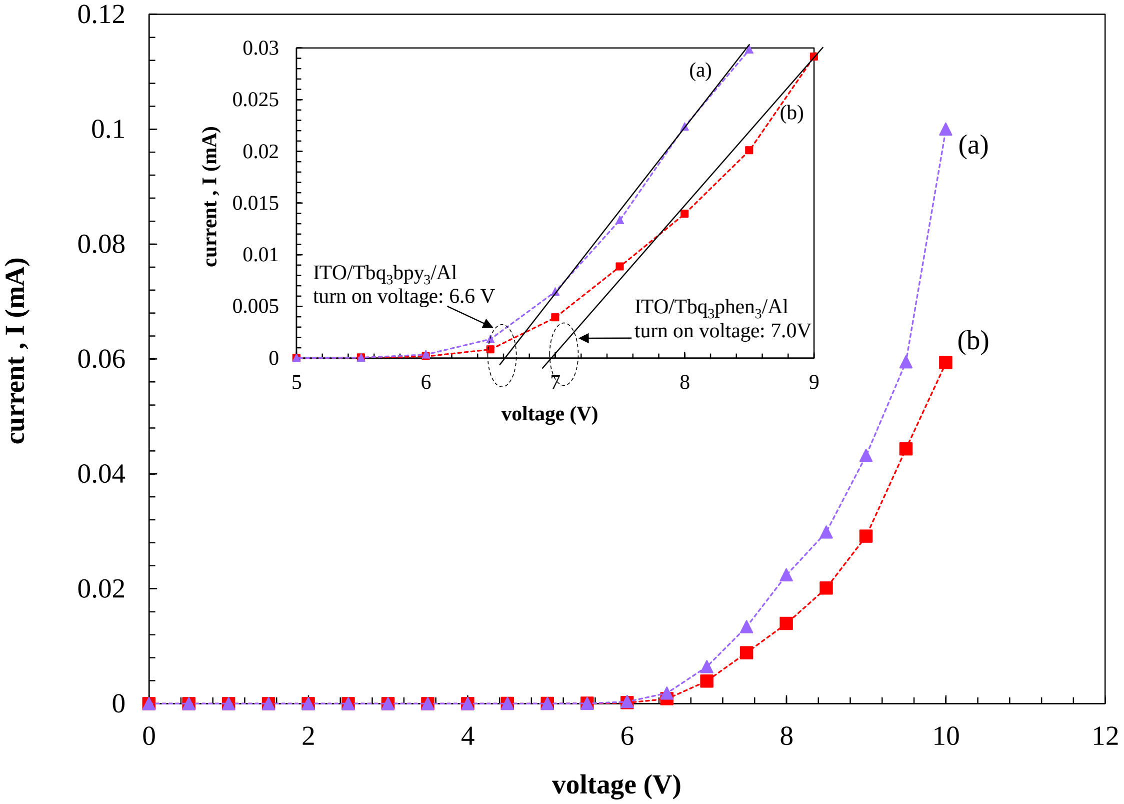

Figure 6.9 I-V characteristics of single layer devices of (a) ITO/ Tbq_3bpy_3/Al, (b) ITO/ Tbq_3phen_3/Al

The variation in the turn on voltage produced by both devices indicates that the I-V characteristics could be affected by adduction of different neutral ligand. Additionally, the highest current observed by ITO/ Tbq_3bpy_3/Al device is 0.10 ± 0.01 mA at 10.0 ± 0.1 V while ITO/ Tbq_3phen_3/Al device produces the highest current, *I* of 0.06 ± 0.01 mA at 10.0 ± 0.1 V. Nonetheless, the device performance is still unsatisfactory due to a considerably low current which may most probably due to a poor charge injection within the organic layer resulting in inefficient charge transport.

The luminance behaviors as a function of applied voltage for both devices are also measured simultaneously with the current. It is well known that the luminescence from terbium complexes devices will produce a green light emission. Nevertheless, such emission is not expected to be observed from ITO/Tbq_3bpy_3/Al and ITO/Tbq_3phen_3/Al devices. This behavior is in accordance to the aforementioned Euq_3 ternary complexes devices. This is because the PL characteristics of Tbq_3 also demonstrate a significant ligand emission indicating inefficient energy transfer from the ligand to the metal Tb^{3+} ion. Therefore, it is anticipated that the colour emitted from these devices are yellowish green and not pure green in which is originated from the ligand emission. However, there are still no electroluminescence (EL) observed from these devices. The absence of luminance on these devices is arised from the imbalance charge injection resulting in the decreased efficiencies due to the exciton quenching as well as non-radiative recombination of charges occurring at the electrode (Kappaun, et al., 2008). This also support the interpretation from the aforementioned result in which the low current is observed.

6.3.2. Charge transport mechanism of ITO/Tbq_3 ternary complexes/Al structure Contact limited versus bulk limited

In order to make the first prediction of the possible bulk-limited behavior in the ITO/ Tbq_3 ternary complexes/Al devices, the I-V characteristics has been fitted in accordance to the power law relations described by, $I \backsim V^m$ where m is determine from the slope. As shown in Figure 6.10 and 6.11, the double logarithmic I-V plots of both devices can be divided into three distinct regions (I-III) with obvious different slope. Interestingly, the fitting results indicate that the slope in these three regions is more than 2 (m>2), suggesting the presence of trap distribution in these devices. The absence of the other two theories which are ohmic and SCLC currents indicates that the trap distribution might occur at the electrode. This is also serves as a support to the emission quenching predicted in the last section in which will lead to a non-radiative emission in OLED. Therefore, it is confirmed that the observed I-V characteristics are not bulk-limited.

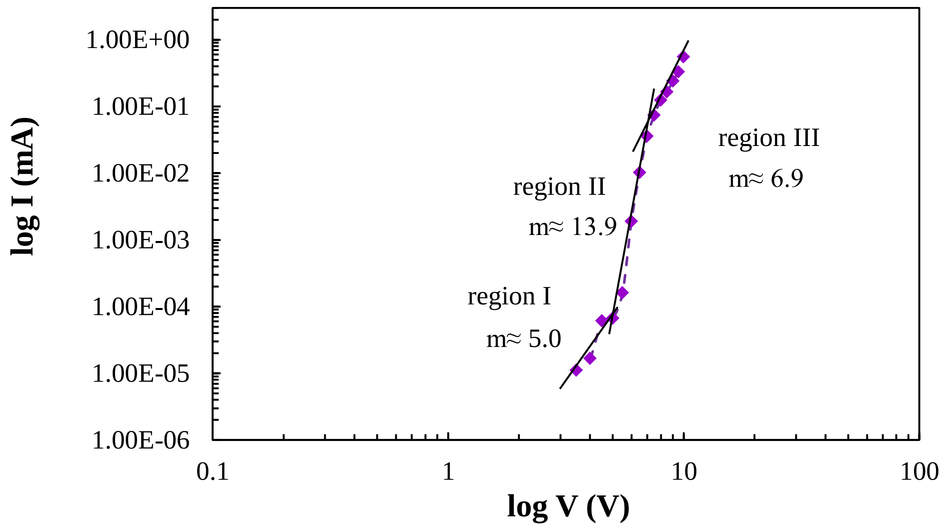

Figure 6.10 Logarithmic plot of I-V characteristic of ITO/Tbq_3bpy_3/Al

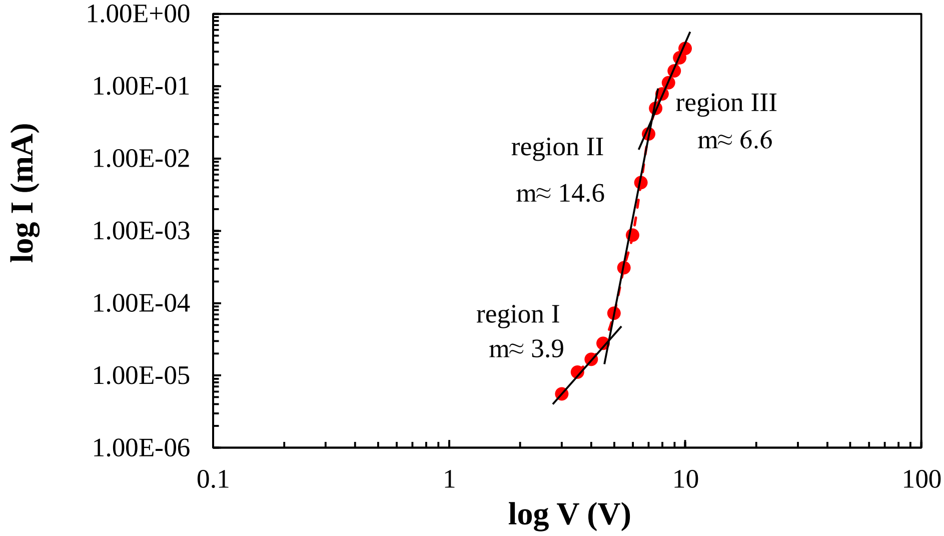

Figure 6.11 Logarithmic plot of I-V characteristic ITO/Tbq_3phen_3/Al

The variation of the slopes might represent the different trapping behavior such as slow, fast, shallow and deep trap. However, these phenomenons will not be discussed in this dissertation as the main objective of this fitting is just to verify the involvement of the bulk limited in the transport mechanism.

The presence of the contact-limited effect in these devices is approximated by R-S thermionic emission which assumes that the injection at metal and organic layer interface is thermally activated at the room temperature. In order to determine the R-S behavior, a plot of ln I~$V^{1/2}$ is evaluate in the lower voltage region. The characteristics of ln I~$V^{1/2}$ in the lower voltage region for both devices are demonstrated in Figure 6.12. From these plots, it is seen that R-S effect model is linearly well fitted. Therefore, the contact-limited model is predicted to dominate the transport mechanism in the ITO/ Tbq_3 ternary complexes/Al devices. It is also noteworthy that the detail explanation on the R-S plot is not further analyzed as it is only meant to predict the R-S behavior.

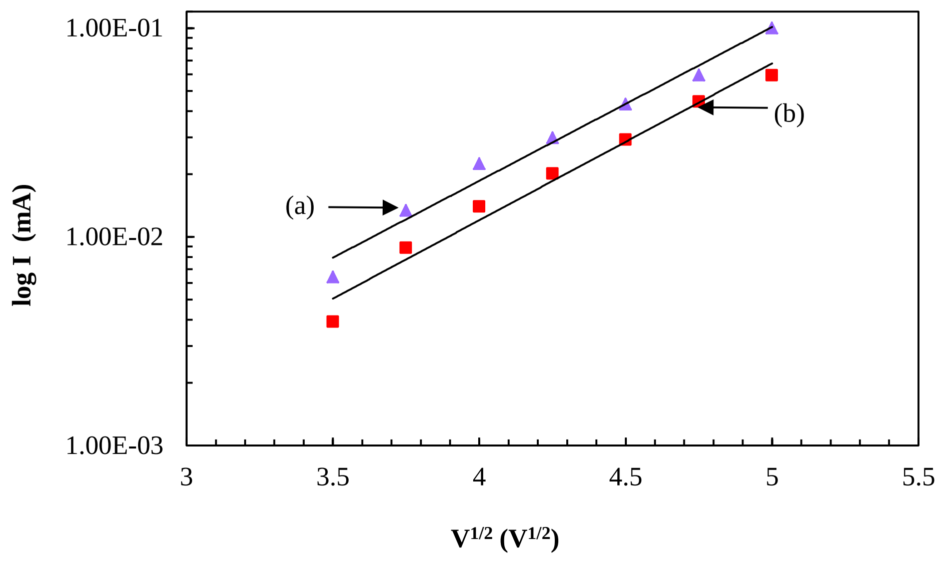

Figure 6.12 Richardson-Schottky plot of I- V characteristics of (a) ITO/Tbq_3bpy_3/Al and (b) ITO/ Tbq_3phen_3/Al

It is also observed that the adduction of the neutral ligand does not play a significant role in determining the transport properties as both complexes demonstrate the occurrence of the contact-limited behavior. It can be proposed that the transport behavior does not influence by the properties of the Tbq_3 ternary complexes as the bulk material. This behavior is in accordance to the aforementioned Euq_3 ternary complexes behavior which further support the dominance of the contact limited effect but not the bulk limited effect.

6.3.3. Evaluation of electronic parameters for the ITO/Tbq_3 ternary complexes/Al structure

In order to further asses the proposed model which is the contact limited, the electrical characteristics of the ITO/Tbq_3 ternary complexes/Al devices is further analyzed by taking the assumption that the formation of Schottky barrier height at the Al/Tbq_3 ternary complexes junction (Günsel, et al., 2011). Several electronic parameters are extracted from the experimental data of the semi-logarithmic I-V characteristics which is described by the exponential expression of the Shockley equation as expressed in Equation (6.1) (Aydin, et al., 2011; Farag, et al., 2011; G. Wetzelaer, et al., 2011).

The semi-logarithmic I-V plots of ITO/Tbq_3bpy_3/Al and ITO/Tbq_3phen_3/Al devices are shown in Figure 6.13. It is noticeable in this figure that the semi-logarithmic I-V plots demonstrate rectifying properties in which is reflected from the exponential rise of the current at the lower voltage as shown in the region I. This behavior may cause by the decrease in the depletion region layer at the junction interface (Güllü, et al., 2008; Günsel, et al., 2011; Shah, et al., 2011). As the voltage increases, the current starts to deviate from the linear exponential due to the effect of series resistance, R_s from the contact wires or bulk resistance of the organic layer, the interfacial layer and the interfaces state which is significant in the downward concave curvature in the semi-logarithmic I-V characteristic (Farag, et al., 2011; Güllü, et al., 2008). The non-ideal behavior exhibits by these devices permits the extraction of the electronic parameters such as the ideality factor, n, effective barrier height, Φ_b and saturation current, I_0. According to Equation (6.4), the ideality factor, n, can be obtained from the slope of the semi-logarithmic I-V plots. The ideality factor, n as high as 16.993± 0.004 and 18.837± 0.003 have been calculated for ITO/Tbq_3bpy_3/Al and ITO/Tbq_3phen_3/Al devices respectively. As expected, the ideality factors, n also deviate from unity. The reason for the high values has been explained in the previous section.

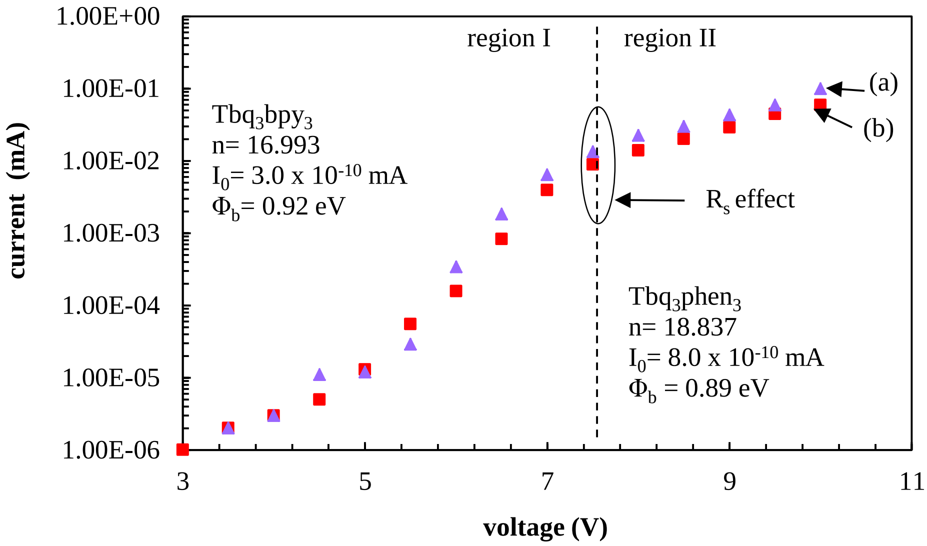

Figure 6.13 I- V characteristics of single layer devices of (a) ITO/Tbq_3bpy_3/Al and (b) ITO/ Tbq_3phen_3/Al

The saturation current, I_0 is calculated from the intercept of the exponential part of the linear region of semi-logarithmic I-V characteristics (Aydin, et al., 2011; Boyarbay, et al., 2008; Farag, et al., 2008; Farag, et al., 2011; Günsel, et al., 2011) The saturation current, I_0 for ITO/Tbq_3phen_3/Al and ITO/Tbq_3bpy_3/Al yields the value of (8.0± 0.1) x10^{-10} mA and (3.0± 0.1) x10^{-10} mA respectively. The saturation current, I_o is then used in Equation (6.5) to obtain the effective barrier height, Φ_b. The calculated effective barrier height, Φ_b for Tbq_3phen_3/Al and Tbq_3bpy_3/Al junctions are found to be 0.89 ± 0.01 eV and 0.92 ± 0.03 eV respectively. The inverse relationship between the effective barrier height, Φ_b and the ideality factor, n is also observed which appears to be in accordance with the aforementioned ITO/Euq$_3$phen$_3$/Al and ITO/Euq$_3$bpy$_3$/Al as well.

Figure 6.14 shows the plots of dV/d (ln I)-I of the Cheung's functions. According to Equation (6.6) the series resistance, R_s and the ideality factor, n are obtained from the slope and y-axis intercept of the dV/d (ln I)-I plot. The obtained values for series resistance, R_s for ITO/Tbq$_3$bpy$_3$/Al and ITO/Tbq$_3$phen$_3$/Al were found to be 48.6 ± 0.2 kΩ and 58.1 ± 0.2 kΩ respectively. On the other hand, the ideality factor, n is obtained as 16.715 ± 0.001 and 14.598 ± 0.003 for ITO/Tbq$_3$phen$_3$/Al and ITO/Tbq$_3$bpy$_3$/Al respectively. These values are considerably greater than the values calculated using conventional I-V method. As explained previously, the deviation is probably due to the existence of the series resistance, interface states and the voltage drop across the interfacial layer (Shah, et al., 2011).

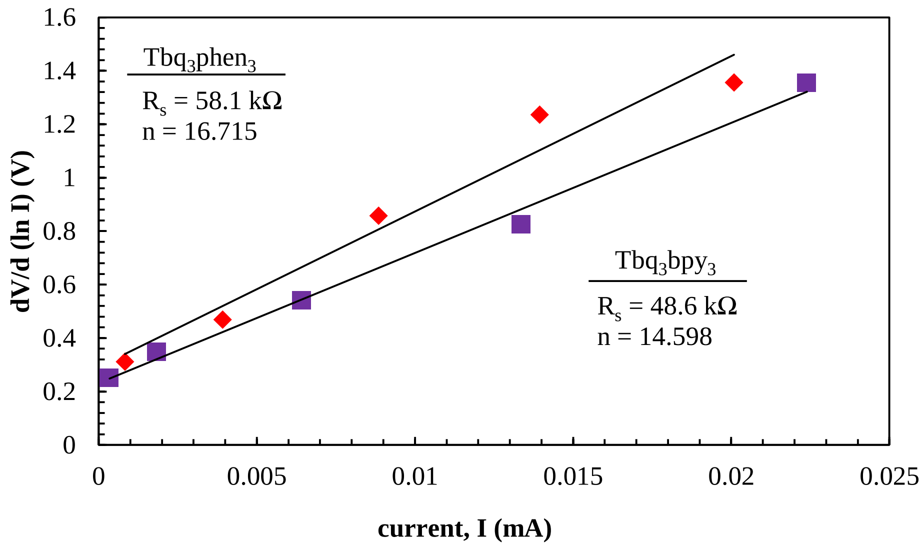

Figure 6.14 dV/d(ln I)- I plot of single layer devices of (a) ITO/Tbq$_3$bpy$_3$/Al and (b) ITO/ Tbq$_3$phen$_3$/Al

The H(I)-I characteristics is then plotted according to the Equation (6.13) as indicated in Figure 6.15. Again the series resistance, R_s and effective barrier height, Φ_b can be determined from the slope and y-axis intercept of the plot as given in Equation (6.8)

(Farag, et al., 2011; Shah, et al., 2011). The series resistance value for ITO/ Tbq_3bpy_3/Al and ITO/Tbq_3phen_3/Al were found to be 51.2 ± 0.4 kΩ and 52.2 ± 0.4 kΩ. It is noticeable that series resistance, R_s values determined from the H(I)-I plot are approximately closed to the values obtained from the dV/d (lnI)-I plot. This describes that the Cheung's functions is appropriate for the determination of the series resistance, R_s. On the other hand, the effective barrier heights, Φ_b, obtained for ITO/ Tbq_3bpy_3/Al and ITO/Tbq_3phen_3/Al were found to be 0.86 ± 0.03 eV and 0.75 ± 0.02 eV. The obtained values for the effective barrier height, Φ_b of both devices are also closed to the values measured from the conventional I-V method. This shows that the utilization of the Cheung's function is valid for the determination of the barrier height, Φ_b.

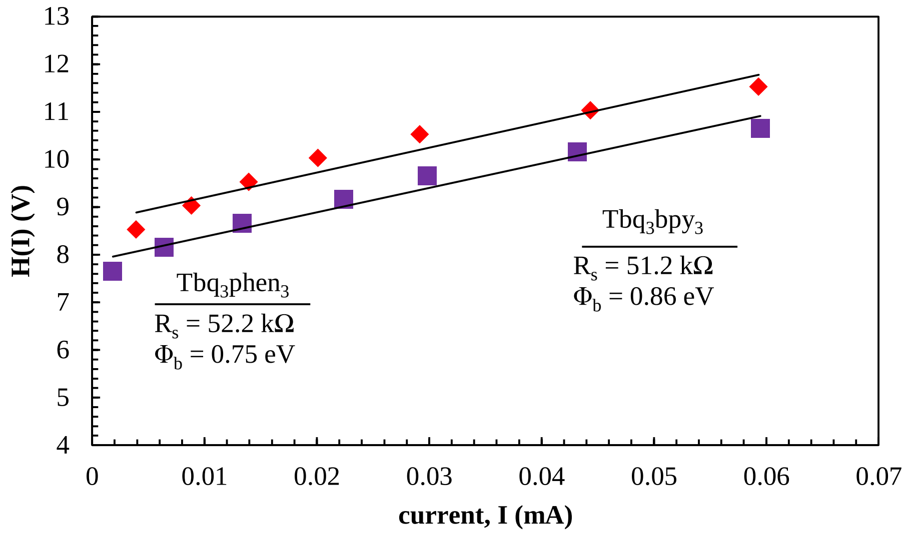

Figure 6.15 H(I)- I plot of single layer devices of (a) ITO/Tbq_3bpy_3/Al and (b) ITO/Tbq_3phen_3/Al

For clarification, all the diode parameters extracted from both conventional I-V method and Cheung's function are tabulated in Table 6.2. In contrast to the Euq_3 ternary complexes, the saturation current I_o is found to be very small and in agreement with the values obtained by other organic semiconductor behavior which are typically in the range 10^{-10}- 10^{-12}.Other than that, the effective barrier height, Φ_b is found in the range from 0.75- 0.92 eV. These values was too high to allow ohmic state which requires the barrier height, Φ_b to be less than 0.3 eV (Crone, et al., 1998). This may cause the injected current to be insufficient to deliver the maximum possible SCLC in the material. Therefore the bulk limited is not suitable to explain the transport characteristics of these materials which further provide additional support for the dominance of the contact-limited transport model in these devices.

Table 6.2 Various parameters extracted from the I- V characteristics of ITO/Tbq_3phen_3/Al and ITO/Tbq_3bpy_3/Al

Diode parameter	ln I- V method		Cheung's functions			
			dV/d(ln I) - I		H(I)-I	
	Tbq_3phen_3	Tbq_3bpy_3	Tbq_3phen_3	Tbq_3bpy_3	Tbq_3phen_3	Tbq_3bpy_3
I_0 (mA)	$(8.0 \pm 0.1) \times 10^{-10}$	$(3.0 \pm 0.1) \times 10^{-10}$	-	-	-	-
Φ (eV)	0.89 ± 0.01	0.92 ± 0.03	-	-	0.75± 0.02	0.86 ± 0.03
n	18.837 ± 0.003	16.993 ± 0.004	16.715 ± 0.001	14.598 ± 0.003	-	-
R_s (kΩ)	-	-	58.1 ± 0.2	48.6 ± 0.2	52.2 ± 0.4	51.2± 0.4

The predicted value of barrier height, Φ_b as well as the band gap, E_g which has been obtained from Chapter 5 have been utilized to estimate the HOMO and LUMO of the Tbq_3 ternary complexes material. The schematic diagram of these devices is shown in Figure 6.16. It is obvious that the barrier height Φ_b, from the ITO to the Tbq_3bpy_3 and Tbq_3phen_3 organic layers are too large to allow efficient charge injection from the electrode. It is noteworthy that the ideal barrier height for an efficient hole injection is 0.5 eV (Qin, et al., 2012). The barrier height Φ_b, for ITO/Tbq_3bpy_3/Al and

ITO/Tbq_3phen_3/Al which were found to be 1.45 eV and 1.46 eV respectively are considered to be very high to allow efficient injection from the electrode into the bulk material. This will cause the number of injected holes is less than electrons leading to imbalanced charge carrier injection or carrier mobility. Therefore the reduction of the recombination rate of electrons and holes in the organic layer is expected (Jiao, et al., 2011). For this reason, the efficiencies of OLED are also expected to decrease due to the exciton quenching processes close to the electrodes or non-radiatiave recombination of charges at the electrodes (Kappaun, et al., 2008). This would be one of the possible reason for OLED's failure in these devices. Moreover, it is also serves as a support to the domination of the contact-limited transport mechanism in these devices.

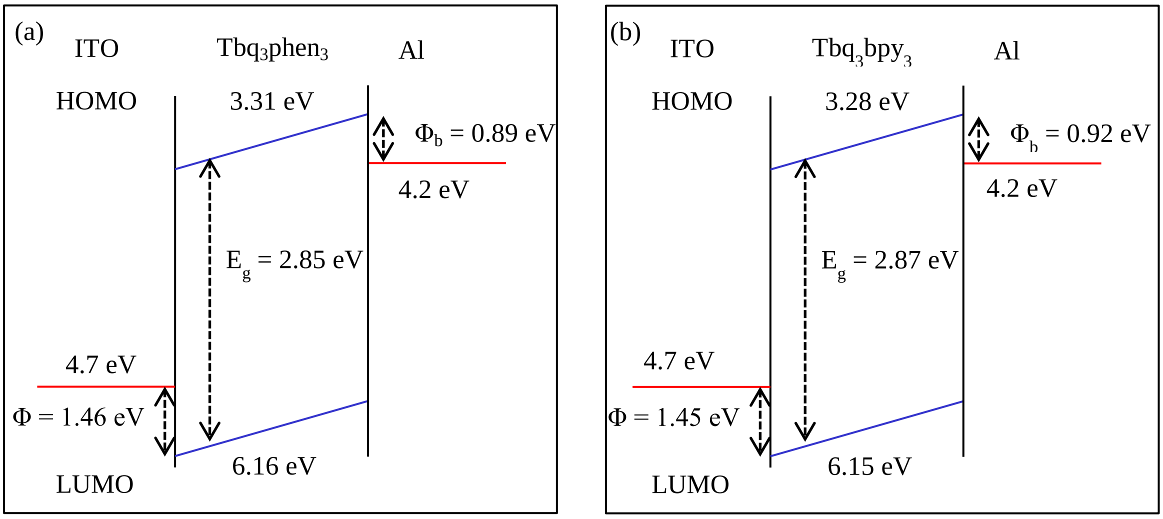

Figure 6.16 Schematic band diagrams of (a) ITO/ Tbq_3phen_3/Al and (b) ITO/ Tbq_3bpy_3/Al after contact

The ideality factor, n also exhibits an inverse relationship with the effective barrier height, Φ_b in which can be reflected by the increment of the barrier height, Φ_b and the reduction of the ideality factor. The higher ideality factor, *n* exhibits by ITO/Tbq_3phen_3/Al compared to that of ITO/Tbq_3bpy_3/Al that is due to the higher series resistance, R_s is also found to be in accordance to the aforementioned Euq_3 ternary complexes devices. This shows that Tbq_3 ternary complexes with Phen ligand will cause a higher resistance and ideality factor compared to that of Bpy ligand. From this finding, it is obvious that the adduction of different neutral ligand can also influenced their electrical properties. This is reflected by the variation in the parameters extracted from the I-V characteristics upon adduction of the neutral ligand.

6.4. Electrical analysis for single layer OLED device with ITO/Req_3 ternary complexes/Al structure: Effect of different metal centre.

6.4.1. I-V characteristics of ITO/Req_3 ternary complexes/Al structure

It has been discovered in the previous section that the adduction of Bpy ligand as the neutral ligand has reduced the turn on voltage of the Tbq_3 ternary complexes device whereas the adduction of Phen ligand as the neutral ligand has reduced the turn on voltage of the Euq_3 ternary complexes device. The voltage exhibits by ITO/Euq_3bpy_3/Al is much lower compared to that of ITO/Tbq_3bpy_3/Al.

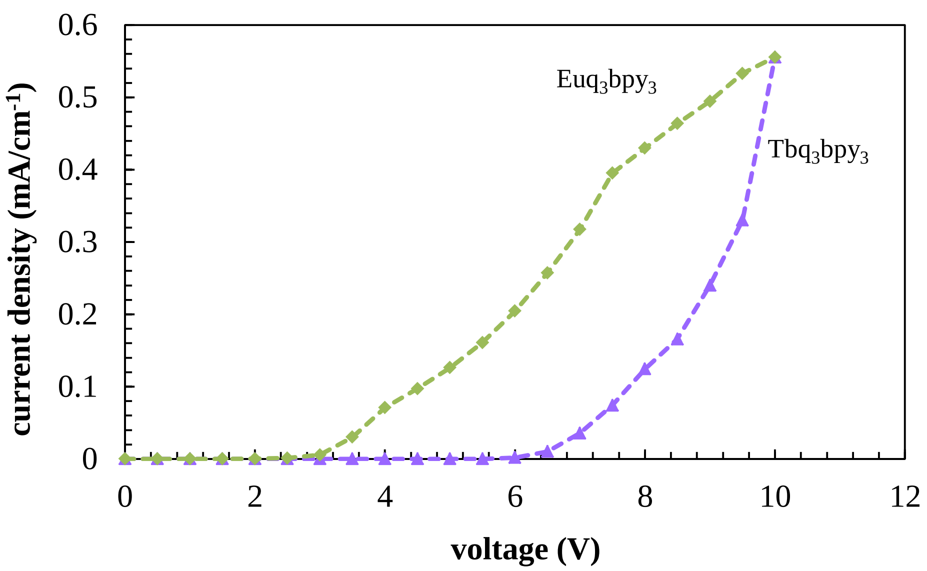

Figure 6.17 I- V characteristics of single layer devices of ITO/Euq_3bpy_3/Al and ITO/Tbq_3bpy_3/Al

In accordance to such effect, it is obvious that the neutral ligand plays a significant role in the electrical properties of these devices, affecting the turn on voltage. Nevertheless, the effect of rare earth metal to the electrical properties is not yet discussed. In order to foresee some insight into the metal effect, the I-V characteristics of the Eu^{3+} and Tb^{3+} ternary complexes are compared based on the same neutral ligand. The I-V characteristics of the ITO/Euq_3bpy_3/Al and ITO/Tbq_3bpy_3/Al devices are shown in Figure 6.17. It was found that the turn on

The same trend was also observed for ITO/Euq_3phen_3/Al and ITO/Tbq_3phen/Al devices (Figure 6.18) in which the turn on voltage of the Euq_3 ternary complexes demonstrate a slightly lower voltage compare to that of Tbq_3 ternary complexes. As pointed out in the Chapter 5, the high atomic radius of the rare earth metal will cause a stronger electronic effect which consequently will cause the enhancement of the π–π orbital stacking (Muhammad, Abdul Hapip, & Sulaiman, 2010). The increase in the π–π orbital stacking will lead to the enhancement of the delocalization of charge carrier. It is known that the electrons in the *π* bond can be delocalized via conjugation with neighboring *π* bonds, thus giving rise to charge carrier mobility.

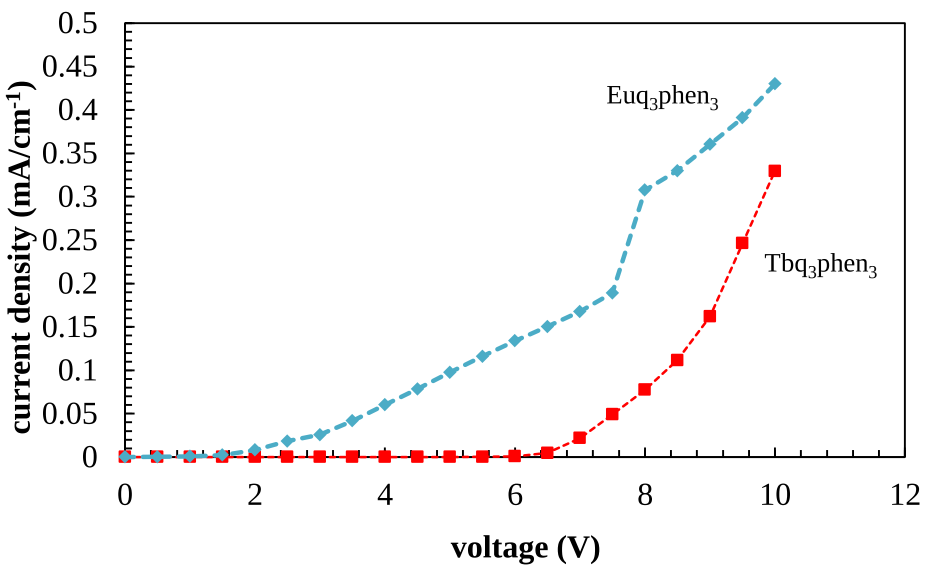

Figure 6.18 I- V characteristics of single layer devices of ITO/Euq_3phen_3/Al and ITO/Tbq_3phen_3/Al

For this reason, the charge transport of the Euq_3 ternary complexes will be more effective in accordance to the increase in the charge hopping along the π orbital. Additionally, the electrical conductivity experienced by Eu^{3+} which is $1.1x10^{-6}$ Sm^{-1} is slightly higher compare to that of Tb^{3+} which is $0.9x10^{-6}$ Sm^{-1}. This may explains the good operating characteristics of the Euq_3 ternary complex devices, in which can be reflected by the low turn on voltage.

6.4.2. Charge transport mechanism of ITO/Req_3 ternary complexes/Al structure

The charge transport mechanism of all *ITO/Req_3 ternary complexes/Al* has been well fitted to the theory proposed by the contact limited in which is represented by R-S model. This implies that the effect of different rare earth metals which supposedly to contribute to different properties of the organic semiconductor does not influence the transport behavior. This finding also supported the domination of the contact limited since it does not depends on the material properties as compared to that of the bulk material.

6.4.3. Evaluation of electronics parameter for the with ITO/Req_3 ternary complexes/Al structure

In order to study the effect of different rare earth metals, the electrical parameters of Tbq_3 and Euq_3 ternary complexes with Bpy and Phen as the neutral ligand is tabulated in Table 6.3 and 6.4 as for clarification and assessment. From Table 6.3, it can be observed that a linear relationship between the ideality factor, n and the barrier height, Φ_b for both complexes exists. Such behavior appears to contradict the inverse relationship between the ideality factor, n and the barrier height, Φ_b obtained from section *6.2.3* and *6.3.3.* According to Aydin the correlation between the ideality factor, n and the barrier height, Φ_b varied from diode to diode (Aydin, Akkiliç, & Kiliçoğlu, 2004). He attributes the linear dependence of the ideality factor, *n* and the barrier height, Φ_b to the lateral inhomogeneities of the barrier height (Aydin, et al., 2004). In comparison with Euq_3 ternary complex, Tbq_3 ternary complex is found to exhibit a larger ideality factor, n with an increase of the barrier height, Φ_b. The higher ideality factor, *n* obtained for Tbq_3 ternary complex is further supported by the higher series resistance, R_s estimated from this complex. Other than that, it is also observed that the saturation current, I_o of Tbq_3 ternary complexes is relatively lower compare to that of Euq_3 ternary complexes indicating the charges that are able to overcome the barrier height barrier are much smaller in magnitude compare to the Euq_3 ternary complexes.

Table 6.3 Various parameters extracted from the I- V characteristics of ITO/Euq_3bpy_3/Al and ITO/ Tbq_3bpy_3/Al

Diode parameter	ln I- V method		Cheung's functions			
			dV/d(ln I) - I		H(I)-I	
	Euq_3bpy_3	Tbq_3bpy_3	Euq_3bpy_3	Tbq_3bpy_3	Euq_3bpy_3	Tbq_3bpy_3
I_0 (mA)	(7.0± 0.1) x 10^{-7}	(3.0± 0.1) x 10^{-10}	-	-	-	-
Φ (eV)	0.72 ± 0.03	0.92 ± 0.03	-	-	0.79± 0.03	0.86± 0.03
n	16.638 ± 0.001	16.993 ± 0.004	11.689 ± 0.003	14.598 ± 0.003	-	-
R_s (kΩ)	-	-	24.7 ± 0.3	48.6 ± 0.2	28.7± 0.5	51.2± 0.4

Table 6.4 presents various parameter extracted for Euq_3 and Tbq_3 ternary complexes with Phen as the neutral ligand. It is also noticed that both conventional ln I-V and Cheung's method shows that the Tbq_3 ternary complexes exhibits a larger ideality

factor, n as the barrier height Φ_b increases. This behavior is also in accordance with the aforementioned Tbq_3 ternary complexes with Bpy ligand. This finding further support the effect of different rare earth metals is expected to established a linear relationship between the ideality factor, n and the barrier height, Φ_b. In addition, the ideality factor, *n* exhibited by Tbq_3 ternary complexes are found to be larger compare to the Euq_3 ternary complexes. This is further supported by the higher series resistance, R_s showed by Tbq_3 ternary complexes compare to that of Euq_3 ternary complexes. The saturation current, I_o for Tbq_3 ternary complexes was also found to be smaller compared to the Euq_3 ternary complexes. This behavior was found to be in accordance to the Tbq_3 ternary complexes with Bpy ligand. This indicates that all Tbq_3 ternary complexes possess much smaller charge carrier that is able to overcome the barrier compare to that of Euq_3 ternary complexes, despite of different neutral ligand.

Table 6.4 Various parameters extracted from the I-V characteristics of ITO/Euq_3phen_3/Al and ITO/Tbq_3phen_3/Al

Diode parameter	ln I- V method		Cheung's functions			
			dV/d(ln I) - I		H(I)-I	
	Euq_3phen_3	Tbq_3phen_3	Euq_3phen_3	Tbq_3phen_3	Euq_3phen_3	Tbq_3phen_3
I_0 (mA)	(2.0± 0.1) x 10^{-5}	(8.0± 0.1) x 10^{-10}	-	-	-	-
Φ (eV)	0.64± 0.08	0.89± 0.01	-	-	0.68± 0.02	0.75± 0.02
n	17.634 ± 0.001	18.837 ± 0.003	11. 756 ± 0.001	16.715 ± 0.001	-	-
R_s (kΩ)	-	-	59.3 ± 0.4	58.1± 0.2	61.9± 0.5	52.2 ± 0.4

From the above analysis, it is obvious that the adduction of different rare earth metals are also play a significant role in affecting the electrical properties of the ITO/Req_3 ternary complexes/Al devices at the contact. The lower values of the ideality factor, n possess by the Euq_3 ternary complexes indicates a good operating characteristics of the Euq_3 ternary complex devices which further support by the low turn on voltage of the ITO/Euq_3 ternary complexes/Al devices compare to that of the ITO/Tbq_3 ternary complexes/Al devices.

6.5. Conclusion

The I-V characteristics of all devices exhibited a typical diode characteristic with no obvious light emission capture in these single layer devices. The presence of the contact limited as the charge transport mechanism is confirmed from the linear dependence of the Richardson- Schottky plot (ln I-$V^{1/2}$) in the lower voltage region. Further assessment on the Richardson-Schottky plot provides reasonable estimation on the important electronic parameters such as ideality factor, I_o, effective barrier height, Φ_b, ideality factor, n and series resistance, R_s in which are extracted from both conventional ln I- V and Cheung's methods. From the estimation electronic parameters, it can be concluded that the adduction of Phen ligand will result in an enhancement in the ideality factor, n as well as the series resistance, R_s compare to that of Bpy ligand. On the other hand, Euq_3 ternary complexes will experience the lower ideality factor, n and series resistance, R_s compare to that of Tbq_3 ternary complexes. The proposed band diagram prove that the predicted effective barrier height, Φ_b is not an appropriate barrier for an efficient charge injection into the bulk material which further support the domination of the contact limited transport mechanism in these devices.